Available online at www.sciencedirect.com
ScienceDirect
Catalysis Today 126 (2007) 430–435
CATALYSIS TODAY
www.elsevier.com/locate/cattod

Synthesis of CeO_2–MnO_x mixed oxides and catalytic performance under oxygen-rich condition

Xiaodong Wu *, Qing Liang, Duan Weng, Jun Fan, Rui Ran

Laboratory of Advanced Materials, Department of Materials Science and Engineering, Tsinghua University, Beijing 100084, China

Available online 13 July 2007

Abstract

$Ce_{0.5}Zr_{0.5}O_2$, $Ce_{0.5}Zr_{0.2}Mn_{0.3}O_2$ and $Ce_{0.5}Mn_{0.5}O_2$ were prepared by citric acid sol–gel method. The effect of manganese on the structural and redox properties of ceria-based mixed oxides was investigated by means of powder X-ray diffraction, X-ray photoelectron spectroscopy, Brunauer–Emmett–Teller analyses, temperature-programmed reduction and catalytic activity evaluation in the presence of excess O_2. The results showed that some Mn cations could enter into the ceria lattice to form solid solutions. Mn_3O_4 appeared due to the instability of the mixed oxides with increment of the Mn doping ratio while another oxide Mn_2O_3 is detected in the physical mixture of ceria and manganese oxide. These Mn-doped mixed oxides, especially $Ce_{0.5}Mn_{0.5}O_2$, presented better catalytic activities than $Ce_{0.5}Zr_{0.5}O_2$ and even Pt-loaded catalyst for total oxidation of C_3H_8 and oxidative sorption of NO in the presence of excess oxygen. The oxidation ability of Mn and the strong interaction between Mn and Ce were suggested to promote the oxygen storage/transport capacity of the mixed oxides as well as reactive adsorption of nitric oxide and hydrocarbons.

Keywords: Ceria-based mixed oxides; Manganese; Redox; Diesel exhaust

1. Introduction

Catalytic purification of diesel exhaust with excess oxygen has been receiving considerable attention these years. There is a strong demand for the development of new, high efficiency, low-cost materials as active and efficient catalysts for the total oxidation of hydrocarbon (HC) and partial reduction of nitrogen oxides (NO_x). Ceria-based mixed oxides, especially CeO_2–ZrO_2, serve as key materials for the outstanding oxygen storage capacity (OSC) and redox properties. They have been widely used in three-way catalysts (TWCs) for removal of emissions from gasoline engine [1–5].

One of the important routes to improve the catalytic performances of ceria-based mixed oxides is by doping and modification with other elements. Particular attention is being paid to manganese oxides which present good oxidation ability due to several oxidation states of manganese species. CeO_2–MnO_x mixed oxides have been investigated as catalysts in different fields, such as absorption and reaction of NO_x [6–8], selective catalytic reduction of NO_x with NH_3 at low temperature in the presence of excess oxygen [7–9] and catalytic wet oxidation of organic compounds [10,11]. The effect of doping a small quantity of Mn (the doping ratio $x = 0.05$) into CeO_2–ZrO_2 on the total oxidation of methane and light hydrocarbons has also been investigated [12]. These researches show that ionic defects are created by a charge compensation mechanism due to the presence of Mn^{x+} ($x = 2, 3, 4$) with a different charge. In addition, catalytic activity could take advantages from the oxidation ability of Mn and their redox efficiency at low temperature.

In order to study the possible synergetic effect of OSC of ceria and oxidation ability of manganese oxides, we doped a large quantity of manganese into ceria–zirconia mixed oxides and analyzed in detail the catalytic behaviour in the oxidation of C_3H_8 and conversion of NO. Special attention was paid on the structural properties, redox performance and catalytic activity of the mixed oxides. Powder X-ray diffraction, X-ray photoelectron spectroscopy, surface area and temperature-programmed reduction measurements were performed to pursue this aim.

* Corresponding author. Tel.: +86 10 62792375; fax: +86 10 62772726.
E-mail address: wuxiaodong@tsinghua.edu.cn (X. Wu).

0920-5861/$ – see front matter © 2007 Elsevier B.V. All rights reserved.
doi:10.1016/j.cattod.2007.06.014

2. Experimental

2.1. Catalyst preparation

The nominal $Ce_{0.5}Zr_{0.5}O_2$ (CZ), $Ce_{0.5}Zr_{0.2}Mn_{0.3}O_2$ (CZM) and $Ce_{0.5}Mn_{0.5}O_2$ (CM) samples were prepared by citric acid sol–gel method. The nitrates $Ce(NO_3)_3{\cdot}6H_2O$, $Zr(NO_3)_4{\cdot}5H_2O$ and $Mn(NO_3)_2{\cdot}6H_2O$ were mixed according to the ratio of Ce:Mn:Zr = 5:5–*x*:*x* (*x* = 0, 3, 5). Citric acid was added as the complexing agent with a 1.3:1 ratio of citric acid to metal ions including Ce^{3+}, Zr^{4+}, and Mn^{2+}. Then an appropriate amount of polyglycol was added. The blended solution was sufficiently mixed in a magnetic stirrer and heated at 80 °C till forming transparent gel. The resulting gel was dried at 110 °C to receive the brown powders. The present powders were submitted to decomposition at 300 °C for 1 h and calcination at 700 °C for 3 h under a static air in a muffle. The powders were cooled to room temperature (RT) in the furnace. Comparatively, a physical mixed sample was obtained by mixing CeO_2 and MnO_x powders which had been prepared by the same citric acid routine. The atom ratio of Ce:Mn was 1:1. 0.5 wt.% Pt was loaded on the $Ce_{0.5}Zr_{0.5}O_2$ powders by impregnation (Pt/CZ), followed by calcination at 500 °C for 3 h in a muffle.

2.2. Surface characterization

The powder X-ray diffraction (XRD) experiments were performed on a Japan Science D/max-RB diffractometer employing Cu Kα radiation (λ = 1.5418 Å). The X-ray tube was operated at 40 kV and 120 mA. The X-ray powder diffractogram was recorded at 0.02° intervals in the range of $20^\circ \leq 2\theta \leq 80^\circ$ with 3 s count accumulation per step. The identification of the phase was made with the help of the JCPDS cards (Joint Committee on Powder Diffraction Standards). The specific surface areas of the samples were estimated using the N_2 adsorption isotherm at −196 °C by the one-point Brunauer–Emmett–Teller (BET) method using an automatic surface analyzer (Quantachrome NOVA instrument). The samples were degassed in flowing N_2 at 200 °C for 2 h. The X-ray photoelectron spectroscopy (XPS) experiments were carried out on a PHI-5300 ESCA system with Al Kα radiation under UHV (1.33×10^{-8} Pa), calibrated internally by the carbon deposit C1s binding energy (BE) at 285 eV. The temperature-programmed reduction (TPR) was carried out on a HPR20 HIDEN catalytic surfaces analyzer. Typically 100 mg of sample was employed. The flow of 5% H_2/He passed through the powders for 40 min at RT as the pre-treatment. The samples were analyzed under flowing H_2 (5% in Ar, 30 ml min^{-1}) from RT to 750 °C (10 °C min^{-1}).

2.3. Activity measurement

The powder catalyst sample was weighed for 0.5 g and mixed homogeneously with appropriate volume of coarse quartz particles to 3 ml. The mixture was loaded in a quartz reaction tube with the diameter of 10 mm. The catalytic activity was evaluated in a tube micro-reactor by passing a gas mixture simulated to exhaust from diesel engine. The simulated exhaust contained a mixture of O_2 (10%), C_3H_8 (0.02%), NO (0.05%), CO_2 (8%) and N_2 (balance). The concentrations of C_3H_8 and NO were determined on-line by a five-component analyzer SIBENCH (SIEMENS, Germany) with infrared sensor for CO, CO_2, NO, HC and electrochemical sensor for O_2. For the light-off experiments, the reactor was heated from 150 to 650 °C in the flow stream at a gas space velocity of 50 000 h^{-1}.

3. Results and discussion

3.1. Structure and textural properties

Structural features of the mixed oxides were examined by XRD and the result is shown in Fig. 1. All the ceria-based materials crystallize in a fluorite-like cubic phase. No peaks of zirconia are observed in the diffraction pattern of $Ce_{0.5}Zr_{0.2}Mn_{0.3}O_2$ or $Ce_{0.5}Zr_{0.5}O_2$. That means all the Zr cations have dissolved in the ceria lattice. Weak peaks of tetragonal structured Mn_3O_4 are detected in the diffraction pattern of $Ce_{0.5}Zr_{0.2}Mn_{0.3}O_2$ while intensified peaks of Mn_3O_4 appear in the diffraction pattern of $Ce_{0.5}Mn_{0.5}O_2$. It has been reported in the literature [6,9,12] that part of Mn cations could be incorporated into the ceria lattice to form solid solutions and part of Mn cations have been left on the surface of the mixed oxides as finely dispersed Mn_3O_4. This doping method substantially affects the oxidation state of manganese since only Mn_2O_3 phase is detected in the diffraction pattern of the CeO_2/Mn_2O_3 mixture. Thus it is concluded that there should be some strong interaction between manganese oxide and ceria both in the bulk and on the surface for the chemical mixed oxides.

Table 1 gives the structural and textural properties of the samples derived from the XRD, BET and XPS results. As we know, the insertion of smaller cations such as Zr^{4+} (the ionic radius, *r* = 0.84 Å), Mn^{4+} (0.56 Å) and Mn^{3+} (0.62 Å) into the ceria lattice and occupation of the positions of Ce cations (0.97 and 0.114 Å for Ce^{4+} and Ce^{3+}, respectively) results in a contraction of the cell parameter. As reported in the literature

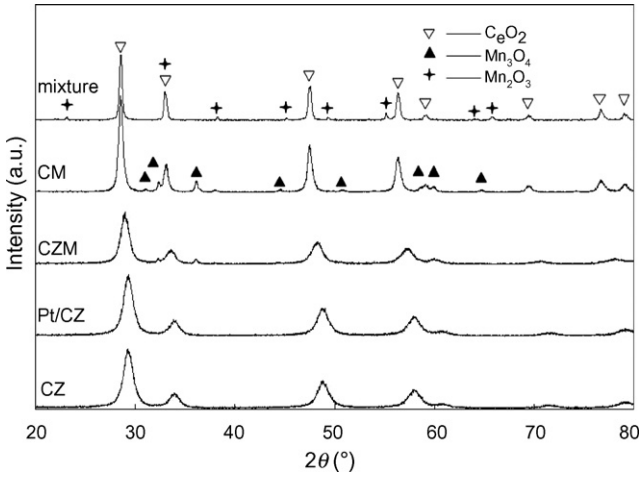

Fig. 1. XRD patterns of the samples.

Table 1
Structure and textural properties of the samples

Sample	a (Å)	BET surface area (m^2/g)	Surface composition (at.%) determined by XPS			
			Ce	Zr	Mn	O
$Ce_{0.5}Zr_{0.5}O_2$	5.273	42.8	9.63	17.63	–	72.73
$Pt/Ce_{0.5}Zr_{0.5}O_2$[a]	5.275	36.4	/	/	/	/
$Ce_{0.5}Zr_{0.2}Mn_{0.3}O_2$	5.334	10.8	12.93	7.23	7.51	72.37
$Ce_{0.5}Mn_{0.5}O_2$	5.410	7.5	10.82	–	13.91	75.27
CeO_2/Mn_2O_3 mixture[a]	5.414	23.6	/	/	/	/

[a] XPS measurement was not performed on the Pt-loaded and physical mixed oxides samples.

[9], the calculated lattice parameter of $Ce_{0.5}Mn_{0.5}O_2$ and CeO_2 was 5.412 and 5.418 Å, respectively. Similarly, the a value of $Ce_{0.5}Mn_{0.5}O_2$ and CeO_2 in the physical mixture is 5.410 and 5.414 Å, respectively in this work, suggesting that some Mn cations have been incorporated into the ceria lattice to form solid solutions. However, there is a great difference of lattice parameters between the Zr- and Mn-doped samples. It is most likely caused by the different solid solubility of zirconia and manganese oxide in the crystal cell of ceria. A cubic solid solution can be maintained even up to 75 at.% zirconia [13] while only a small part of Mn cations can dissolve into the ceria lattice [12]. In addition, the lattice parameter of the Pt-loaded sample is slightly larger than that of pure $Ce_{0.5}Zr_{0.5}O_2$ support. The occurrence of this expansion implies a strong metal–support interaction (SMSI) between platinum and ceria–zirconia solid solutions, causing conversion of the Ce^{4+} to larger Ce^{3+} cations [14].

The surface area of the samples decreases as the Mn content increases (Table 1). According to the literature [12], it is related to the formation of the large MnO_x particles whose surface area is much smaller. Obviously, the contribution of small solid solution crystals to the surface area is more significant than that of MnO_x particles. Similarly, the relative large surface area of the physical mixed oxides arises mainly from ceria. The decreased surface area of Pt-supported sample may be ascribed to its additional calcination process after impregnation.

XPS measurements were performed to further study the surface composition and oxidation states of cerium and manganese in the mixed oxides. It is seen from Table 1 that the Ce/Zr atomic ratios of $Ce_{0.5}Zr_{0.5}O_2$ and $Ce_{0.5}Zr_{0.2}Mn_{0.3}O_2$ are lower than the theoretic values, which implies a formation of Zr-rich phase at the periphery of the particles. On the other hand, the Ce/Mn ratio of $Ce_{0.5}Zr_{0.2}Mn_{0.3}O_2$ is similar to the theoretic value while that of $Ce_{0.5}Mn_{0.5}O_2$ is much lower due to the segregation of Mn_3O_4 on the surface.

In order to obtain information of oxidation states of the surface elements, the Ce 3d, Mn 2p and O 1s XPS spectra were analyzed, respectively. The Ce 3d spectrum can be resolved into eight components [15]. The peaks are assigned for Ce^{4+} as v (882.44–882.58 eV), v'' (888.97–889.21 eV) and v''' (898.35–898.50 eV) for Ce $3d_{5/2}$, with the corresponding Ce $3d_{3/2}$ peaks labelled as u (900.93–901.02 eV), u'' (907.79–907.93 eV) and u''' (916.80–916.84 eV). An additional doublet is also observed due to the presence of Ce^{3+} and is assigned v' (884.59–885.53 eV) and u' (903.33–903.91 eV). It has been proposed that the relative amount of Ce^{4+} can be calculated from the percent area of the u''' peak in the total Ce 3d region [16]. It is seen from Table 2 that the concentration of Ce^{4+} obviously increases with increment of the Mn doping amount. It appears that electrons are transferred from Ce to Mn [17], which is confirmed by the appearance of Mn_3O_4 in the chemical mixture instead of Mn_2O_3 in the physical mixture.

On the other hand, the concentrations of different Mn species were calculated according to the relative area ratio of the Mn $2p_{3/2}$ peaks assigned for Mn^{2+} (640.9 eV), Mn^{3+} (641.8 eV) and Mn^{4+} (642.5 eV) [18]. Fig. 2 shows the Mn 2p region spectra for $Ce_{0.5}Zr_{0.2}Mn_{0.3}O_2$ and $Ce_{0.5}Mn_{0.5}O_2$. Both the Mn $2p_{1/2}$ and Mn $2p_{3/2}$ region were presented as deconvoluted into all its components, and their relative atomic ratios are listed in Table 2. It is interesting that the surface Mn^{4+} atomic ratio increases with increment of the Mn content, which may be ascribed to the very top atomic layer of Mn under oxidative calcination atmosphere. However, it should be taken into account that XPS is basically a surface characterization technique. The oxidation state of manganese in the bulk is very important and remains to be investigated. A metal oxide catalyst possessing numerous oxidation states to facilitate electron transfer processes will be an efficient catalyst for oxidation of hydrocarbon and reduction of NO.

To investigate the oxygen species on the surface, the O 1s spectra were fitted in Fig. 3. The O 1s spectra are fitted with two peak contributions. The primary band (529.4–529.7 eV) denoted as O_{latt} represents the characteristic of lattice oxygen bound to metal cations of the structure, while the additional band (531.6–532.2 eV and 532.9–533.8 eV) belongs most likely to adsorbed oxygen and hydroxyl group, referred to as chemisorbed oxygen [14]. The relative percentages of these two oxygen species are quantified based on the area ratios of O_{latt} and O_{ads} peaks. The proportion of $O_{ads}/(O_{ads} + O_{latt})$ of $Ce_{0.5}Mn_{0.5}O_2$ (40.0 at.%) is higher than that of $Ce_{0.5}Zr_{0.5}O_2$ (37.4 at.%) and $Ce_{0.5}Zr_{0.2}Mn_{0.3}O_2$ (29.0 at.%). This should be due to the high adsorption ability of well-dispersed manganese oxides on the surface, which play as active sites to chemisorb oxygen.

Table 2
Surface composition of the Ce and Mn species derived by XPS

Sample	Ce $3d_{5/2}$ (at.%)		Mn $2p_{3/2}$ (at.%)		
	Ce^{3+}	Ce^{4+}	Mn^{2+}	Mn^{3+}	Mn^{4+}
$Ce_{0.5}Zr_{0.5}O_2$	28.7	71.3	–	–	–
$Ce_{0.5}Zr_{0.2}Mn_{0.3}O_2$	20.2	79.8	49.6	29.4	21.0
$Ce_{0.5}Mn_{0.5}O_2$	18.1	81.9	47.5	17.4	35.1

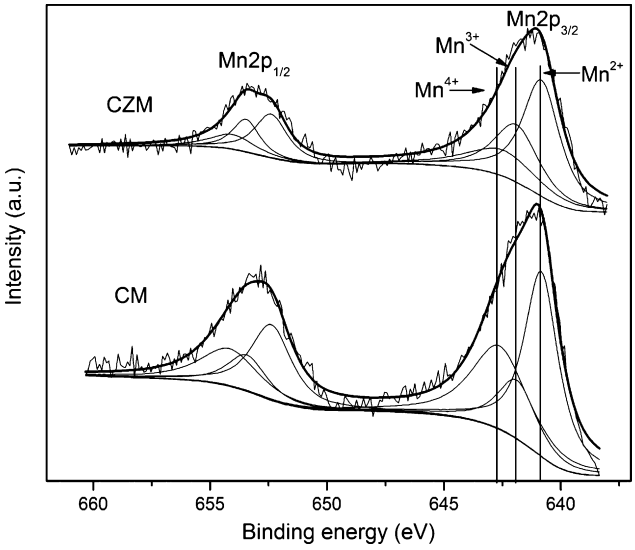

Fig. 2. XPS spectra of Mn 2p for the samples.

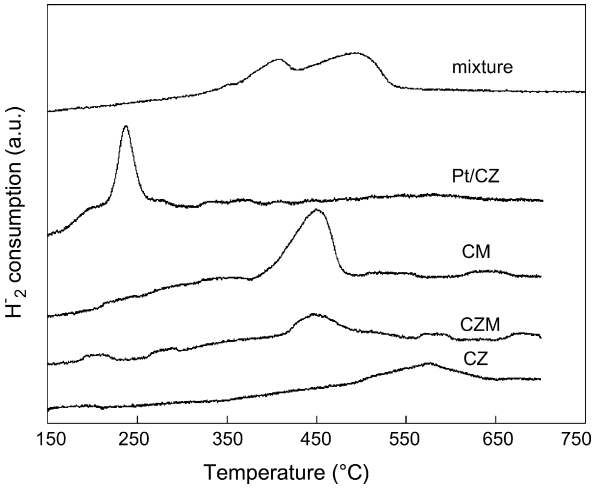

Fig. 4. TPR profiles of the samples.

3.2. Redox and catalytic properties

Fig. 4 shows the TPR profiles of the samples. Typical TPR of ceria usually shows two maxima at ca. 550 and 830 °C, which are associated to surface and bulk reduction, respectively [19]. With the introduction of Zr into the ceria lattice to form $Ce_{0.5}Zr_{0.5}O_2$, the reduction of Ce^{4+} is significantly promoted and it is observed at lower temperatures with a maximum at ca. 580 °C (bulk reduction) and a shoulder at ca. 540 °C (surface reduction). The reduction process is further promoted by Pt through the spillover of hydrogen from platinum species to ceria–zirconia mixed oxides and the subsequent interaction with the support. Its reduction peak is shifted to ca. 237 °C.

Besides the characteristic reduction peak at 580 °C, the maximum peak temperature of $Ce_{0.5}Zr_{0.2}Mn_{0.3}O_2$ is remarkably reduced to ca. 450 °C compared with $Ce_{0.5}Zr_{0.5}O_2$. This phenomenon should be attributed to the introduction of Mn which strongly modifies the reduction behaviour of CeO_2–ZrO_2 mixed oxides. As described in the XRD discussion, some Mn species have been incorporated into the ceria lattice, which create more defectives and bring a higher mobility and diffusion of bulk oxygen. It is easy to find that the maximal reduction peak of $Ce_{0.5}Mn_{0.5}O_2$ is located almost at the same position as that of $Ce_{0.5}Zr_{0.2}Mn_{0.3}O_2$, but its peak area is much larger. One important factor is that the incorporation of more Mn cations may create more defects in the ceria lattice of $Ce_{0.5}Mn_{0.5}O_2$. In addition, Mn element itself possesses active redox behaviour since it exists in several oxidation states. Thus, the shoulder peak of pure manganese oxide at ca. 430 °C or even lower temperature can be ascribed to readily reducible, highly dispersed, surface manganese species, i.e. the reduction of Mn_3O_4 to MnO. For the CeO_2/Mn_2O_3 mixture, there are two major peaks. The former peak is centered around 410 °C and is believed to be attributed to both reduction of Mn_2O_3 to form Mn_3O_4, while the latter peak is centered around 495 °C and may be attributed to the reduction of Mn_3O_4 to MnO and CeO_2 to form Ce_2O_3. No peaks are found around 830 °C in the TPR profile of the CeO_2/Mn_2O_3 mixture (not shown), which implies the bulk reduction of CeO_2 is also significantly promoted by mixing Mn species. Thus, some strong interaction is also suggested to exist between manganese oxides and ceria in the physical mixture, which is substantially different from that of the chemical mixed oxides.

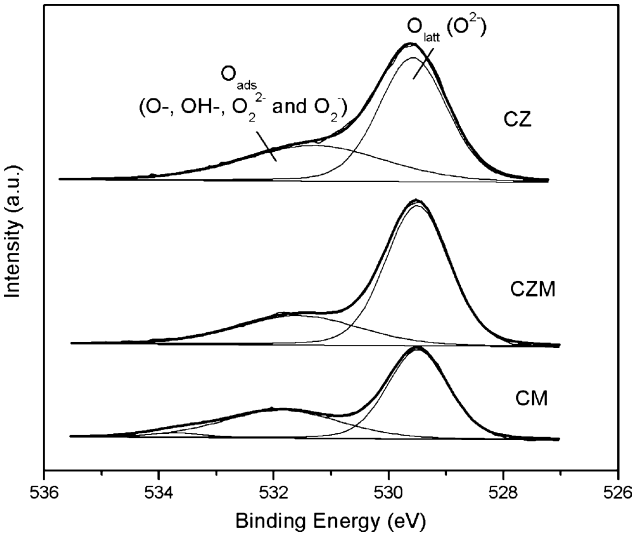

Fig. 3. XPS spectra of O 1s for the samples.

The catalytic activities of the samples under oxygen-rich condition are shown in Fig. 5. None of these catalysts were pretreated before running the reaction. It can be seen that the catalytic ability of total oxidization of propane is significantly improved by doping Mn into ceria. The light-off temperature T_{50} of the CeO_2/Mn_2O_3 mixture (463 °C) is close to that of $Ce_{0.5}Zr_{0.5}O_2$ (470 °C). However, by doping Mn in ceria, T_{50} is sharply decreased down to 342 and 335 °C for $Ce_{0.5}Zr_{0.2}Mn_{0.3}O_2$ and $Ce_{0.5}Mn_{0.5}O_2$, respectively. Even after impregnated with a small amount of platinum (0.5 wt.%) on ceria–zirconia mixed oxides, the T_{50} (374 °C) is still higher than those of Mn-doped samples. In addition, propane is totally oxidized over these Mn-doped samples after 450 °C while the

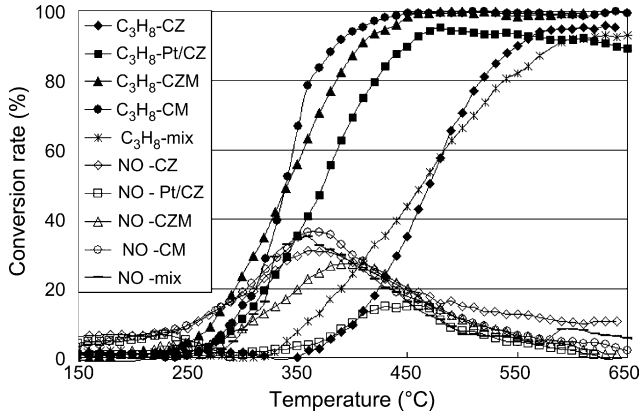

Fig. 5. Catalytic activities of the samples in the presence of excess oxygen.

conversion rate cannot reach 100% over the other catalysts. Thus the Mn-doped ceria-based oxides are suggested to be a good oxidation catalyst for removal of light hydrocarbons.

Under diesel conditions, the reduction of NO is not favoured. It is seen from Fig. 5 that a NO conversion window is observed for all the samples between 250 and 500 °C, especially displaying a maximal conversion rate of 37% at 370 °C for $Ce_{0.5}Mn_{0.5}O_2$. The mixed oxides can be classified in descending order of $Ce_{0.5}Mn_{0.5}O_2$ (251 °C) > $Ce_{0.5}Zr_{0.5}O_2$ (257 °C) > CeO_2/Mn_2O_3 mixture (305 °C) > $Ce_{0.5}Zr_{0.2}Mn_{0.3}O_2$ (310 °C) > $Pt/Ce_{0.5}Zr_{0.5}O_2$ (396 °C) when looking at the onset temperature of NO conversion T_{10}. It is noted that the Pt-supported ceria–zirconia shows ''the worst activity'' for NO conversion in the presence of excess oxygen, which may be due to the sintering of Pt during the catalyst preparation and activity measurement.

It is interesting to compare the activity of $Ce_{0.5}Mn_{0.5}O_2$ with that of the CeO_2/Mn_2O_3 mixture. Propane conversion reaches 100% at 420 °C over $Ce_{0.5}Mn_{0.5}O_2$ while it is still not completed at 650 °C over the mixture. The reactive adsorption capacity of organic deposits on the surface of mixed CeO_2–Mn_3O_4 phase has also been found to be substantially high [20]. The oxidative activity can benefit to a large extent from well-dispersed surface manganese oxides which behave as active oxidation catalysts. Both Mn_3O_4 and Mn_2O_3 can absorb oxygen and act, in an oxidizing atmosphere, like p-type semiconductors [21]. On the other hand, it has been suggested that the catalysis for hydrocarbon oxidation is not exclusively surface sensitive, but bulk effect has also much importance [22]. A bulk effect such as bulk oxygen diffusion should be the main responsibility for the enhancement in catalytic activity when Mn cations are doped into ceria. O_2^- (superoxide) and O_2^{2-} (peroxide), serving as strong oxidants, may be formed on $Ce_{0.5}Mn_{0.5}O_2$ as the result of activation of oxygen subsequent to O_2 adsorption. The interaction between Ce and Mn greatly improves the oxygen storage capacity as well as oxygen mobility on the surface of the catalyst. This can facilitate the reactive absorption of nitric oxide and the oxidation of propane.

Thus, the better catalytic behaviour of $Ce_{0.5}Mn_{0.5}O_2$ may be ascribed to two major considerations: (i) the presence of CeO_2–MnO_x solid solutions and (ii) the active redox properties of well-dispersed Mn_3O_4 on the surface. The synergetic mechanism may be explained by the following simplified reactions:

$$NO(g) \xrightarrow{O^*} NO_2(a) \xrightarrow{O^*} NO_3(a) \quad (1)$$

$$C_3H_8(g) \rightarrow C_3H_8(a) \quad (2)$$

$$NO_2(a)/NO_3(a) + C_3H_8(a) \rightarrow N_2(g) + CO_2(g) + H_2O(g) \quad (3)$$

The incorporation of Mn within the ceria lattice may bring a lot of lattice defects and enhance the mobility of lattice oxygen to the surface to be activated. Gaseous NO may first react with surface active oxygen species (O*) bound to Mn to form NO_2 or even NO_3 adsorbates in the presence of excess oxygen [23], which then coordinate to a Ce^{4+}–O^{2-} pair in an adjacent site. The random distribution of Mn and Ce in the fluorite lattice appears to be effective in producing a large number of pair sites for oxidative sorption of NO. Soon after this, the nitrite/nitrate species can be reduced by C_3H_8, which may be dissociatively adsorbed onto surface Mn species and subsequently spills over onto the adjacent ceria. In our study, a similar NO conversion window has been observed in the gas mixture of NO + O_2 + CO_2 + N_2 but none in the reaction system of NO + CO_2 + N_2 (not shown), which confirms this oxidative sorption mechanism.

4. Conclusion

The results show that, compared with $Ce_{0.5}Zr_{0.5}O_2$ and the corresponding Pt-loaded catalyst, $Ce_{0.5}Mn_{0.5}O_2$ is a superior catalyst for the total oxidation of C_3H_8 and oxidative sorption of NO in the presence of excess oxygen. The catalyst yields a total oxidation of C_3H_8 at 450 °C and a maximal NO conversion of 37% at 370 °C under a GHSV = 50 000 h^{-1}. It can be attributed to the synergetic effect of CeO_2–MnO_2 solid solutions and well-dispersed Mn_3O_4 species, i.e. the activation of oxygen, oxidative sorption of NO, reactive adsorption of C_3H_8 and their interactions.

Acknowledgements

The authors would like to acknowledge Projects 2004CB719503 supported by the Ministry of Science and Technology of China and Project 50502023 supported by National Natural Science Foundation of China. Moreover, we would also thank Research Center for Eco-Environmental Sciences, Chinese Academy of Sciences for performing TPR experiments and Key Lab of Advanced Materials, Tsinghua University.

References

[1] H.S. Gandhi, G.W. Graham, R.W. McCabe, J. Catal. 216 (2003) 433.
[2] H.W. Jen, G.W. Graham, W. Chun, R.W. McCabe, J.P. Cuif, S.E. Deutsch, O. Touret, Catal. Today 50 (1999) 309.
[3] H. Muraki, G. Zhang, Catal. Today 63 (2000) 337.
[4] R. Flouty, E. Abi-Aad, S. Siffert, A. Aboukaïs, Appl. Catal. B: Environ. 46 (2003) 145.

[5] J.R. Mellor, A.N. Palazov, B.S. Grigorova, J.F. Greyling, K. Reddy, M.P. Letsoalo, J.H. Marsh, Catal. Today 72 (2002) 145.
[6] M. Machida, M. Uto, D. Kurogi, T. Kijima, Chem. Mater. 12 (2000) 3158.
[7] M. Machida, D. Kurogi, T. Kijima, Catal. Today 84 (2003) 201.
[8] M. Machida, D. Kurogi, T. Kijima, J. Phys. Chem. B 107 (2003) 196.
[9] G. Qi, R.T. Yang, J. Phys. Chem. B 108 (2004) 15738.
[10] G. Qi, R.T. Yang, J. Catal. 217 (2003) 434.
[11] G. Qi, R.T. Yang, R. Chang, Appl. Catal. B: Environ. 51 (2004) 93.
[12] G. Blanco, M.A. Cauqui, J.J. Delgado, A. Galtayries, J.A. Pérez-Omil, J.M. Rodríguez-Izquierdo, Surf. Interf. Anal. 36 (2004) 752.
[13] A.E. Nelsona, K.H. Schulzb, Appl. Surf. Sci. 210 (2003) 206.
[14] X.D. Wu, J. Fan, R. Ran, D. Weng, Chem. Eng. J. 109 (2005) 133.
[15] P. Burroughs, A. Hamnett, A.F. Orchard, G. Thornton, J. Chem. Soc., Dalton Trans. (1976) 1686.
[16] J.Z. Shyu, W.H. Weber, H.S. Gandhi, J. Phys. Chem. 92 (1988) 4964.
[17] H. Chen, A. Sayari, A. Adnot, F. Larachi, Appl. Catal. B: Environ. 32 (2001) 199.
[18] E. López-Navarrete, A. Caballero, A.R. González-Elipe, M. Ocaña, J. Eur. Ceram. Soc. 24 (2004) 3057.
[19] S. Sato, R. Takahashi, T. Sodesawa, N. Honda, J. Mol. Catal. A: Chem. 221 (2004) 177.
[20] M. Abecassis-Wolfovich, M.V. Landau, A. Brenner, M. Herskowitz, Ind. Eng. Chem. Res. 43 (2004) 5089.
[21] M. Baldi, V.S. Escribano, J.M.G. Amores, F. Milella, G. Busca, Appl. Catal. B: Environ. 17 (1998) 175.
[22] E. Finocchio, G. Busca, Catal. Today 70 (2001) 213.
[23] M. Machida, M. Uto, D. Kurogi, T. Kijima, J. Mater. Chem. 11 (2001) 900.